

Article

Immobilization of Phospholipase D for Production of Phosphatidylserine by a Pickering Emulsion Strategy

Hui Sun [†] , Shujing Zhang [†], Dianqing Liu, Zhiqi Huang, Yuxin Ge, Jiayi Hou, Fuping Lu  and Yihan Liu ^{*} 

Key Laboratory of Industrial Fermentation Microbiology, Ministry of Education, Tianjin Key Laboratory of Industrial Microbiology, College of Biotechnology, Tianjin University of Science and Technology, Tianjin 300457, China; huisun26@163.com (H.S.); zsjtust@163.com (S.Z.); liudianqing@mail.tust.edu.cn (D.L.); hhuangzhiqi@163.com (Z.H.); 13223457120@163.com (Y.G.); houjiayi0618@126.com (J.H.); fupinglu_ameel@126.com (F.L.)

* Correspondence: lyh@tust.edu.cn

[†] These authors contributed equally to this work.

Abstract: As a natural phospholipid, phosphatidylserine (PS) plays a key role in the food, cosmetic, and pharmaceutical industries. Recently, substantial attention has been focused on the phospholipase D (PLD)-mediated synthesis of PS. However, the application of free PLD is usually limited by high cost, poor reusability, and low stability. In this study, PLD from *Streptomyces antibioticus* (saPLD) was efficiently immobilized on SiO₂ through physical adsorption to develop saPLD@SiO₂. The stability of the saPLD@SiO₂ was higher than that of the free saPLD over an extensive range of temperature and pH conditions. Furthermore, the PS yield of saPLD@SiO₂ was approximately 41% in the first cycles, and still kept 60% of its initial PS yield after 14 cycles. After a 25-day storage period, the saPLD@SiO₂ retained 62.5% of its initial activity, while the free saPLD retained only 34.3%, suggesting that saPLD@SiO₂ has better stability than free saPLD. A Pickering emulsion was produced by dispersing saPLD@SiO₂ in solutions (ethyl propanoate and acetate/ acetic acid buffer) using ultrasound. The engineered Pickering emulsion demonstrated excellent catalytic activity, with a 62% PS yield after 6 h, while free saPLD had only 18%. The results indicated that a high-performance and sustainable biocatalysis method was established for the effective synthesis of PS.

Keywords: phosphatidylserine; phospholipase D; immobilization; Pickering emulsion



Citation: Sun, H.; Zhang, S.; Liu, D.; Huang, Z.; Ge, Y.; Hou, J.; Lu, F.; Liu, Y. Immobilization of Phospholipase D for Production of Phosphatidylserine by a Pickering Emulsion Strategy.

Catalysts **2023**, *13*, 1318. <https://doi.org/10.3390/catal13101318>

Academic Editor: Evangelos Topakas

Received: 2 July 2023

Revised: 25 August 2023

Accepted: 13 September 2023

Published: 23 September 2023



Copyright: © 2023 by the authors. Licensee MDPI, Basel, Switzerland. This article is an open access article distributed under the terms and conditions of the Creative Commons Attribution (CC BY) license (<https://creativecommons.org/licenses/by/4.0/>).

1. Introduction

Phosphatidylserine (PS) has been widely utilized in the functional food and pharmaceutical industries as a phospholipid ingredient [1]. As a nutritional supplement, PS has been widely added to milk powder, beverages, health products, and so on [2]. PS has also been exploited to treat diseases, including inflammatory diseases, senescence, and Alzheimer's disease [3,4], and it may function as a common biomarker to target tumor cells [5,6]. Additionally, PS can be employed as an essential component of liposomes for the delivery of functional substances [7]. Natural PS is found in animal organs (e.g., bovine brains [8]); however, it may result in the increased risk of disease transmission. Furthermore, natural PS can also be obtained from other sources, such as vegetables, oils, soybeans, and yolks [9]. Although PS can be directly extracted from plants, due to the easy operation and wide range of sources, the preparation cycle is long, and it is difficult to separate and purify the product, leading to the low yield of PS [10]. Therefore, the availability and production of PS from these sources are currently inadequate to meet the increasing demand [11]. Nowadays, the phospholipase D (PLD, EC 3.1.4.4)-mediated enzymatic synthesis of PS has the advantages of simple operation, easy acquisition of raw materials, and environmental friendliness, which has attracted extensive attention [12,13]. Phosphatidylcholine (PC) and L-serine can be exploited as substrates to synthesize PS with a PLD-mediated transphosphatidylation reaction. Up to now, PLDs have been found to

be abundant in plants, animals, and microorganisms [14]. Among all of these sources, the PLDs from *Streptomyces* strains (e.g., *S. antibioticus* [15], *Streptomyces* sp. PMF [16], and *S. chromofuscus* [17]) have drawn lots of attention. Thus, they have been selected as the main catalysts for synthesizing PS, in view of their easier enzyme preparation, broader substrate specificity, and higher transphosphatidylase activity, compared to those of the other sources [18].

Generally, the free PLD activity is remarkably influenced by external environmental factors, including temperature, pH, and material toxicity, which might decrease the PS's synthesis efficiency [19]. Furthermore, the use of the free PLD in practical applications is usually limited by the difficulty of recovering from the reaction system, which might lead to a high processing cost [20]. Comparatively, enzyme immobilization can overcome the drawbacks of the free enzymes [21]. Compared to free enzymes, immobilized enzymes are easier to reuse and are more stable. Nanomaterials, which function as supports for immobilizing enzymes, have drawn a lot of attention recently [22], and the diffusion limitations of the substrates and products of the enzyme reactions could be avoided by the large surface area [23]. As a nanomaterial, SiO₂ is generally applied for enzyme immobilization due to its low cost, low toxicity, excellent chemical amenability, good biocompatibility, and thermostability [24]. For example, lipases from *Burkholderia cepacia* [25], *Candida rugosa* [26], *Yarrowia lipolytica* [27], and *Aspergillus niger* [28] have been immobilized on SiO₂ to have better functions. Considering the stability and sustainable uses, SiO₂-immobilized PLD might provide an approach for synthesizing PS.

Additionally, an organic–water biphasic system is commonly required for enzymatic synthesis of PS, because L-serine is soluble in an aqueous solution, but PC and PS are only soluble in an organic solvent. Therefore, the reaction can only take place at the interface between the water and the organic biphasic system, thus, the limited interfacial area might decrease the PLD efficiency [29]. In recent years, Pickering emulsions have attracted a surge of interest for enzymatic catalysis in biphasic systems, which are generated to stabilize the interface between two immiscible liquids by using solid particles [30]. These solid-particle-stabilized Pickering emulsions can not only shorten the mass transfer distance, but also enlarge the reaction interface area in order to increase biocatalysis in the biphasic system [31]. It has been reported that lipase AYS was adsorbed and immobilized on mesoporous carbon spheres to prepare a Pickering emulsion, which was successfully utilized for the acylation reaction of α -linolenic acid and phytoalcohol [32]. The hydrophobic silica nanoparticles that immobilized lipase from *Candida rugosa* also stabilized the Pickering emulsion and remarkably increased the enzyme activity [33]. However, it still remains difficult to prepare stable Pickering emulsions to synthesize PS with the immobilized PLD as solid pellets.

In this study, PLD from *S. antibioticus* (saPLD) was immobilized on the surface of SiO₂, followed by investigating the optimal immobilization conditions of saPLD. Then, the immobilized saPLD@SiO₂ was identified, and the enzymatic characteristics, such as the thermostability, pH stability, and storage stability, were compared with those of the free saPLD. The operational stability of the saPLD@SiO₂ was also assessed. Moreover, a Pickering emulsion was prepared using ethyl propionate as the medium and saPLD@SiO₂ as the solid particles to facilitate the production of PS.

2. Results and Discussion

2.1. Immobilization Conditions of saPLD

The immobilization conditions of saPLD were explored in the following three aspects: the enzyme content, the immobilization temperature, and the immobilization time. As demonstrated in Figure 1a, the load on the carrier enhanced gradually with the increased enzyme content (0.25–1 U), and the relative enzyme activity and the enzyme activity recovery rate enhanced. When the content of the enzyme was over 0.75 U, the relative enzyme activity and the enzyme activity recovery rate of the saPLD@SiO₂ exhibited a downward trend. The possible reason for this could be that saPLD aggregated as multi-layered on the surface of SiO₂ and enhanced the mass transfer resistance, leading to

the reduced activity of the saPLD@SiO₂. Furthermore, as indicated in Figure 1b, the relative enzyme activity and the enzyme activity recovery rate enhanced with the increased immobilization temperature, and they achieved their maximal values at 20 °C. However, when the immobilization temperature was further enhanced (20–40 °C), the relative enzyme activity and the enzyme activity recovery rate were reduced.

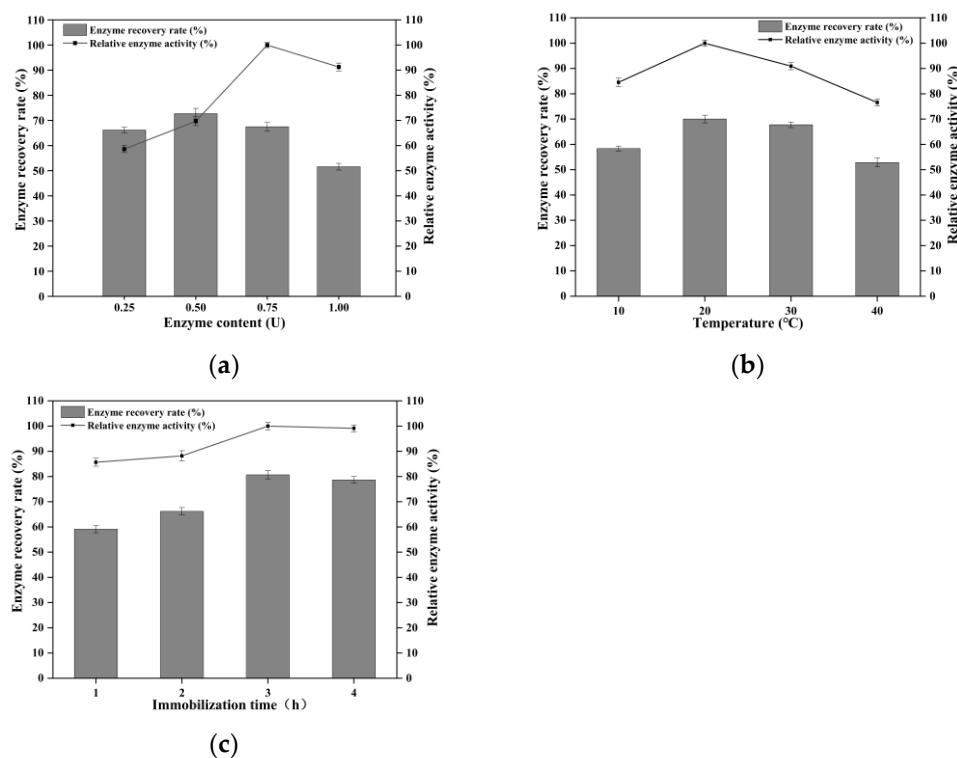


Figure 1. The influence of enzyme content (a), immobilization temperature (b), and immobilization time (c) on the relative enzyme activity and the enzyme activity recovery rate. The data exhibited are the average values obtained from three paralleled experiments, while the error bars stand for the standard deviations.

In addition, the enzyme activity recovery rate and the enzyme activity enhanced with increased immobilization time (1–3 h) (Figure 1c). There were more immobilization sites in the SiO₂ structure in the early stage of immobilization, thus, saPLD could rapidly “occupy” the surface of SiO₂, leading to a rapidly increased immobilization rate [34]. However, the enzyme activity recovery rate and the enzyme activity remained essentially unchanged with the further extended immobilization time (3–4 h). This phenomenon might be explained by the fact that most of the immobilization sites of SiO₂ were “occupied.” In this part, the optimal immobilization time was considered to be 3 h. Compared to other approaches, this nanotechnology had a shorter immobilization time, because it took 12 h to covalently immobilize the PLD to epoxy-based resin [35], and it took 24 h to immobilize the PLD on the supports activated by CNBr [36]. In summary, the optimum immobilization conditions were as follows: the immobilization temperature was 20 °C, the enzyme content was 0.75 U, and the immobilization time was 3 h. Hence, the saPLD@SiO₂ was prepared for further identification and follow-up studies under the optimum conditions.

2.2. Characterization of saPLD@SiO₂

2.2.1. Scanning Electron Microscopy

The surface morphology of the saPLD@SiO₂ was detected using scanning electron microscopy Apreo (SEM). As exhibited in Figure 2, the rough surface of the saPLD@SiO₂, at ×10,000 and ×20,000 magnification, suggested that saPLD was successfully immobilized

onto the surface of SiO_2 . The adequate exposure of saPLD might help to enhance the catalytic efficiency and the catalytic activity of catalyst.

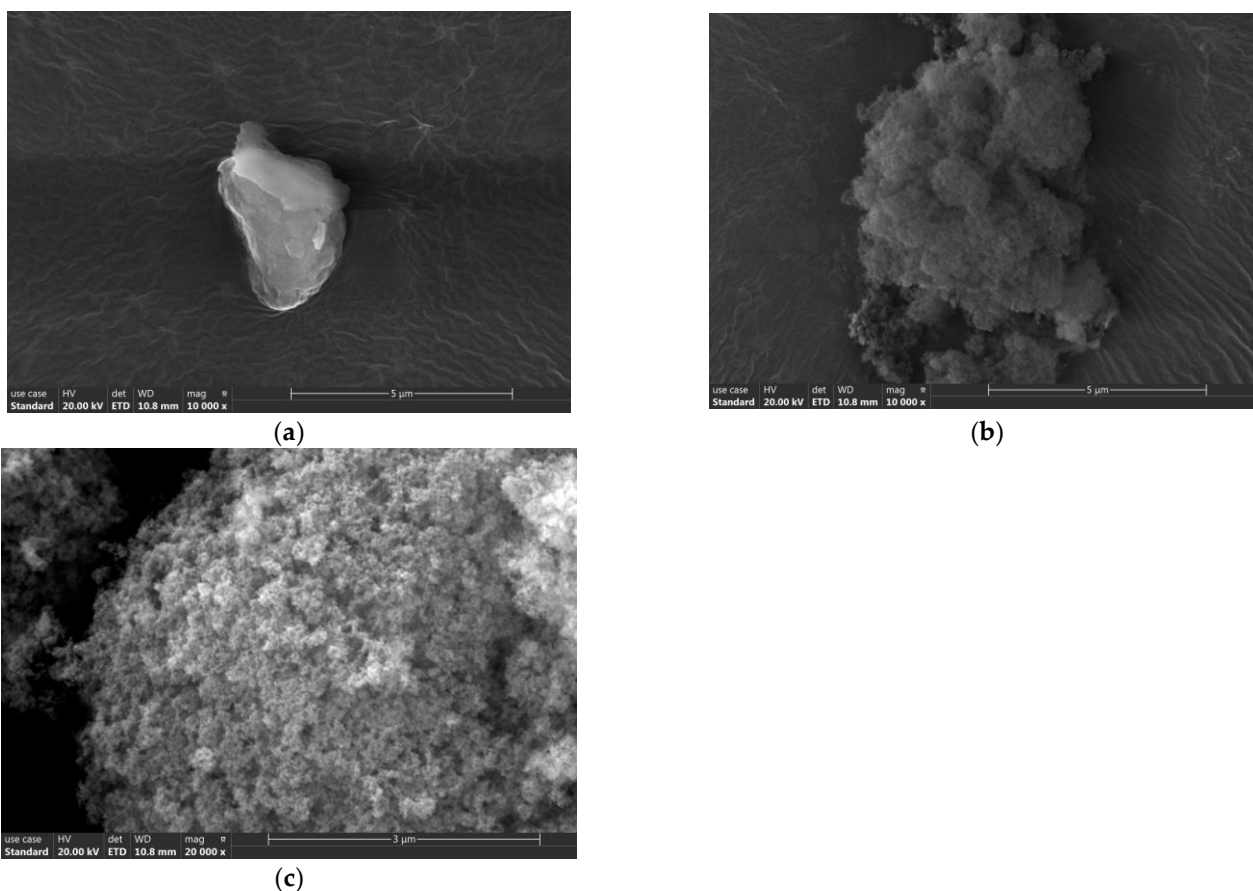


Figure 2. Scanning electron microscopy images of SiO_2 at 10,000 \times magnification (a); saPLD@SiO_2 at 10,000 \times magnification (b); and saPLD@SiO_2 at 20,000 \times magnification (c).

2.2.2. Confocal Laser Scanning Microscopy

To determine the successful immobilization of enzymes on SiO_2 , saPLD and SiO_2 were labeled with fluorescent dyes, and the fluorescence of the saPLD@SiO_2 was detected using confocal laser scanning microscopy (CLSM). On the one hand, the surface of SiO_2 was covered with rhodamine B (RB) by covalent binding [37], and the resulting fluorescent SiO_2 demonstrated a great imaging stability. On the other hand, fluorescein isothiocyanate (FITC) was labeled to saPLD based on the reaction between the carbon–sulfur bond amine on fluorescence and the R-amino group on lysine of the protein to generate a FITC–protein conjugate [38]. As exhibited in Figure 3, the FITC-labeled saPLD displayed green fluorescence, and RB-labeled SiO_2 showed red fluorescence, confirming that the saPLD and SiO_2 were identified. These results indicated that saPLD covered the surface of SiO_2 , suggesting successful immobilization.

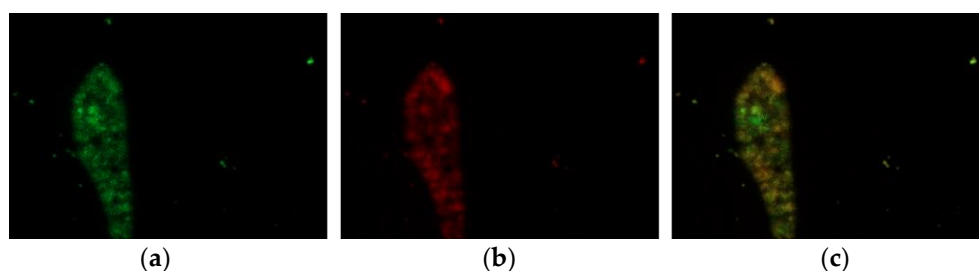


Figure 3. Confocal laser scanning microscopy images of (a) saPLD@SiO₂, including the FITC-labeled saPLD, (b) saPLD@SiO₂ containing RB-labeled SiO₂, and merged image of (c) saPLD@SiO₂ containing FITC-labeled saPLD and RB-labeled SiO₂.

2.2.3. Fourier Transform Infrared Spectroscopy

The chemical ingredients of the saPLD@SiO₂ and SiO₂ were analyzed using Fourier transform infrared spectroscopy (FT-IR). Each functional group or chemical bond of the molecule in the sample correspondingly generate differing absorption and vibration frequencies through the penetration of infrared light [39]. The FT-IR spectra of saPLD@SiO₂ and SiO₂, in wavenumbers of 4000–400 cm⁻¹, are exhibited in Figure 4. The spectrum of SiO₂ was identified by 468 cm⁻¹ of Si–O flexural vibration, 800 cm⁻¹ of Si–O–Si bending vibration, 960 cm⁻¹ of Si–OH bending vibration, 1100 cm⁻¹ of Si–O–Si asymmetric stretching vibration, 1620 cm⁻¹ of O–H bending of absorbed water, and 3427 cm⁻¹ of O–H stretching vibration. The saPLD@SiO₂ demonstrated identical spectra to the original SiO₂, indicating their similar chemical structure. Furthermore, it was observed that the saPLD@SiO₂ showed new peaks at 2564 cm⁻¹ (carboxyl OH stretching vibration) and 1400 cm⁻¹ (C–H bending vibration). The amide 1 band and the amide 2 band are specific wavenumber ranges in the infrared spectrum, used to represent vibration patterns in compounds containing an amide group [40]. The infrared amide 1 band is usually in the range of 1600–1800 cm⁻¹, and the amide 2 band is typically in the range of 1470–1570 cm⁻¹. An increase in the vibration between the amide 1 and amide 2 bands can be seen after the fixation of the saPLD, indicating a change in the protein structure, which could be due to the formation of new interactions between saPLD and SiO₂.

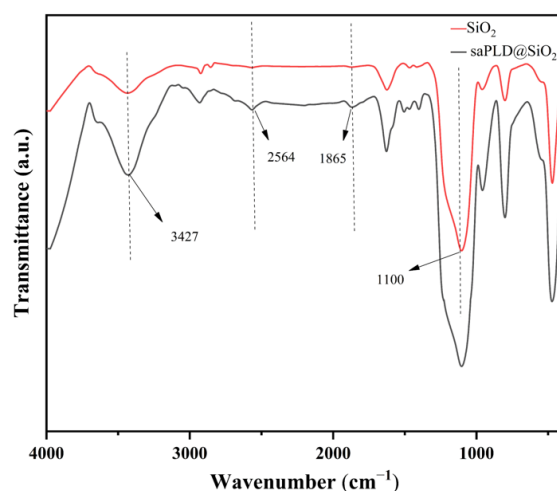


Figure 4. Fourier transform infrared spectra of saPLD@SiO₂ and SiO₂, monitored in wavenumbers of 4000–400 cm⁻¹.

2.3. Properties of saPLD@SiO₂

Although nanomaterials are extensively applied in enzyme immobilization, limited research has been performed on the properties of the immobilization of PLD by nanomateri-

als. Thus, it is critical to analyze the saPLD@SiO₂ properties in the transphosphatidylation reaction, which is conducive to the process of PS production.

2.3.1. Optimum Temperatures and Thermal Stability

As exhibited in Figure 5a, the optimal temperature for both the saPLD@SiO₂ and the free saPLD was 60 °C, but the relative activity of the saPLD@SiO₂ was greater than that of the free saPLD, from 40 °C to 80 °C, indicating that the saPLD@SiO₂ was less affected by the temperature changes than the free saPLD. After incubating at 40 °C and pH 5.5 for 1 h, the free saPLD retained 71% of its initial activity, but the saPLD@SiO₂ retained 91% of its original activity (Figure 5b). After incubating at 50 °C for 1 h, the free saPLD retained only 4.5% residual activity, and incubating at 60 °C for 1 h, the residual activity almost 0%, however, the saPLD@SiO₂ was more stable, and retained 38% and 11% residual activity, respectively (Figure 5b). These phenomena have suggested that the saPLD@SiO₂ showed better tolerance than the free saPLD at different temperatures, which is similar to the PLD (from *Streptomyces* sp.) immobilized on ZnO nanowires/macroporous SiO₂ [41] or the PLD (from *Streptomyces* sp. LD0501) immobilized on SiO₂ [42]. The reason for this might be that the interaction between the support and the enzyme provided a more stable conformation, which could protect the immobilized enzymes at higher temperatures.

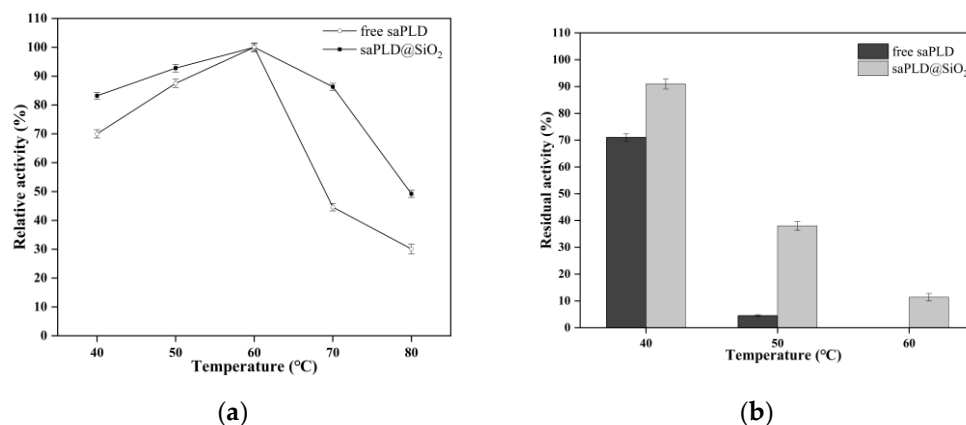


Figure 5. Influence of temperature on the activity (a) and stability (b) of free saPLD and saPLD@SiO₂. The data exhibited are the average values obtained from three paralleled experiments, while the error bars stand for the standard deviations.

2.3.2. Optimum pH and pH Stability

As demonstrated in Figure 6a, the free saPLD had an optimal activity at pH 6.0, whereas the optimal pH for the saPLD@SiO₂ was 7.0. The saPLD@SiO₂ showed a higher relative activity in pH ranging from 5.0 to 9.0, in comparison to the free saPLD. Figure 6b shows that saPLD@SiO₂ has a broader stability range and a higher residual activity than free saPLD at pH 6.0–8.0. After incubating at 4 °C and pH 6.0 for 7 d, the free saPLD retained about 90% of its original activity, while the saPLD@SiO₂ retained nearly 100% of its initial activity. In addition, over 94% of saPLD@SiO₂ maximal activity was detected at pH 7.0–8.0 after 7 days of incubation at 4 °C. However, only 87% and 81% of the highest saPLD activity was observed at pH 7.0 and 8.0, respectively. After being exposed to different pHs for 7 d, it could be seen that the enzyme activity of the saPLD@SiO₂ changed less sharply, indicating that the saPLD@SiO₂ was more stable. This might be due to the fact that the support surface provided protection for the saPLD catalytic sites, making it more efficient in the reaction system with pH changes.

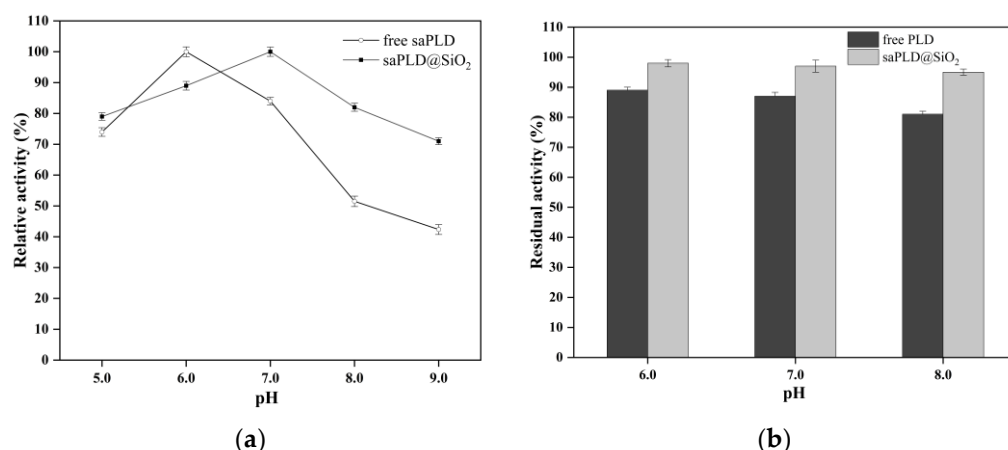


Figure 6. Influence of pH on the activity (a) and stability (b) of free saPLD and saPLD@SiO₂. The data exhibited are the average values obtained from three paralleled experiments, while the error bars stand for the standard deviations.

2.4. Operational Stability of saPLD@SiO₂

Up to now, the transphosphatidylation reaction conducted with free PLD has been reported in many studies. However, the difficulty of reusing the free PLD results in high cost of the enzymatic process. Thus, it is critical to develop immobilized PLD so that it can be reused for practical application in order to reduce the cost. As demonstrated in Figure 7, the PS yield was approximately 41% in the first cycles, and still retained 60% of its initial value after 14 cycles, suggesting that saPLD@SiO₂ has better stability. The loss of PS yield might be due to enzyme deactivation during repeated uses and enzyme leakage during washing. The high operational stability suggested that saPLD@SiO₂ could be applied for producing PS in a continuous system. It has been reported that the saPLD immobilized on epoxy-based resin retained a relative PS yield of 60% after five recycles [35]. Another study showed that the PLD (from *A. radioresistens* a2) immobilized on magnetic nanoparticles coated with SiO₂ could retain 40% of its original activity after eight recycles [43]. In addition, PLD (from *S. halstedii*) was immobilized on the cell surface of *P. pastoris*, and the relative PS yield was still above 40% after four repeated cycles [9].

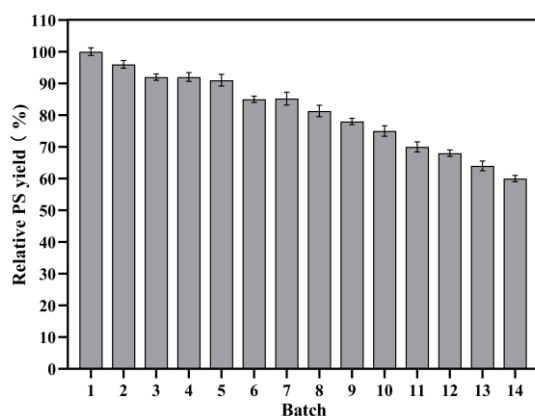


Figure 7. Operational stability of saPLD@SiO₂. The data exhibited are the average values obtained from three paralleled experiments, while the error bars stand for the standard deviations.

2.5. Storage Stability of saPLD@SiO₂

In light of the cost of industrial applications, the storage stability of an enzyme is considered to be the most important factor in immobilization technology. As demonstrated in Figure 8, the residual activity of the free saPLD was 34.3% of its original activity on the 25th day, but the residual activity of the saPLD@SiO₂ was 62.50%. The results are

similar to that of the PLD (from *Streptomyces* sp.) immobilized on epoxy-resin-based hierarchical porous polymers [44]. The storage stability of the enzyme after immobilization was enhanced, in comparison to that of the free enzyme, which might be attributable to the more stable structure of the immobilized enzyme, which enhanced its stability. The increased storage stability would be beneficial to the application and promotion of saPLD@SiO₂ for the synthesis of PS.

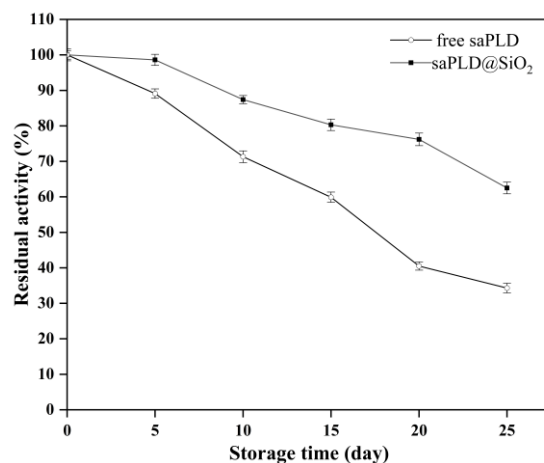
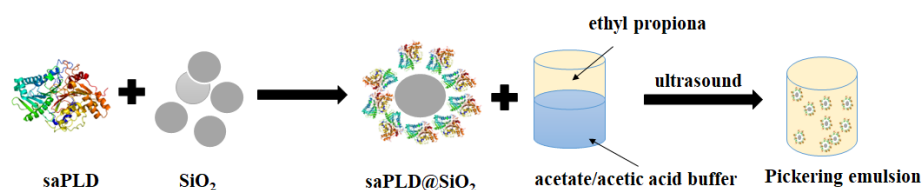


Figure 8. Storage stability of saPLD@SiO₂. The saPLD@SiO₂ and free saPLD were stored at 4 °C for 25 days. The data exhibited are the average values obtained from three paralleled experiments, while the error bars stand for the standard deviations.

2.6. Preparation and Characterization of Pickering Emulsion

PLDs are dissolved in the aqueous phase in conventional methods of synthesizing PS, leading to reduced catalysis kinetics, due to their difficulty to approach PC (in the oil phase) [9]. To overcome this problem, the contact area between the PLD and the substrates (PC and L-serine) can be increased by the emulsion system. In contrary to the surfactant molecules, the particles have a high energy of adsorption, leading to their irreversible adsorption at liquid–liquid interfaces. In a typical Pickering emulsion, the reaction takes place at the oil–water interface, and the emulsion droplets are stabilized by solid particles. Therefore, the Pickering emulsions are usually a stable emulsion system, providing great versatility in two-phase reactions [45]. Pickering emulsions can be water-in-oil, oil-in-water, or even multiple types. Water-in-oil emulsions are generally formed by hydrophobic particles, while stable oil-in-water emulsions are likely to be formed by hydrophilic particles [46]. So far, many techniques have been applied for the preparation of Pickering emulsions, and ultrasound is the most commonly used method [47]. Ultrasound has many advantages, such as good reproducibility, high efficiency, simple operation, and low cost, leading to its extensive application [48]. Additionally, ultrasound can generate a more stable emulsion [49]. Therefore, the Pickering emulsion used in this study was made using ultrasonic treatment.

Scheme 1 demonstrates the working mechanism of preparing the Pickering emulsion. The saPLD@SiO₂ was formed by immobilizing saPLD on SiO₂. Then, the saPLD@SiO₂ was mixed with ethyl propionate and the 20-mM acetate/acetic acid buffer (pH 6.0). Next, the mixture was subjected to ultrasound for 3 min at 40% intensity, with a 3-s ultrasound and a 3-s stand-by, to ultimately prepare the Pickering emulsion. This Pickering emulsion could enhance the interfacial area among the substrates (PC and L-serine) and saPLD@SiO₂, which might lead to an enhanced yield of PS and increase the stability of the emulsion.



Scheme 1. The immobilization of saPLD and preparation of Pickering emulsion.

As demonstrated in Figure 9, the Pickering emulsion was generated by dispersing saPLD@SiO₂ in solutions (5 mL of ethyl propanoate and 5 mL of 20-mM acetate/acetic acid buffer (pH 6.0)) under ultrasound. It was found that the aqueous and organic phases, without sonicating, were clearly stratified, and the saPLD@SiO₂ was suspended in the midst of two phases (Figure 9a). However, the Pickering emulsion formed after sonication showed a more homogeneous texture with no stratification (Figure 9b). After seven days, the Pickering emulsion showed no clear change in its morphological appearance and could still hold its own weight (Figure 9c), indicating that the Pickering emulsion was stable.

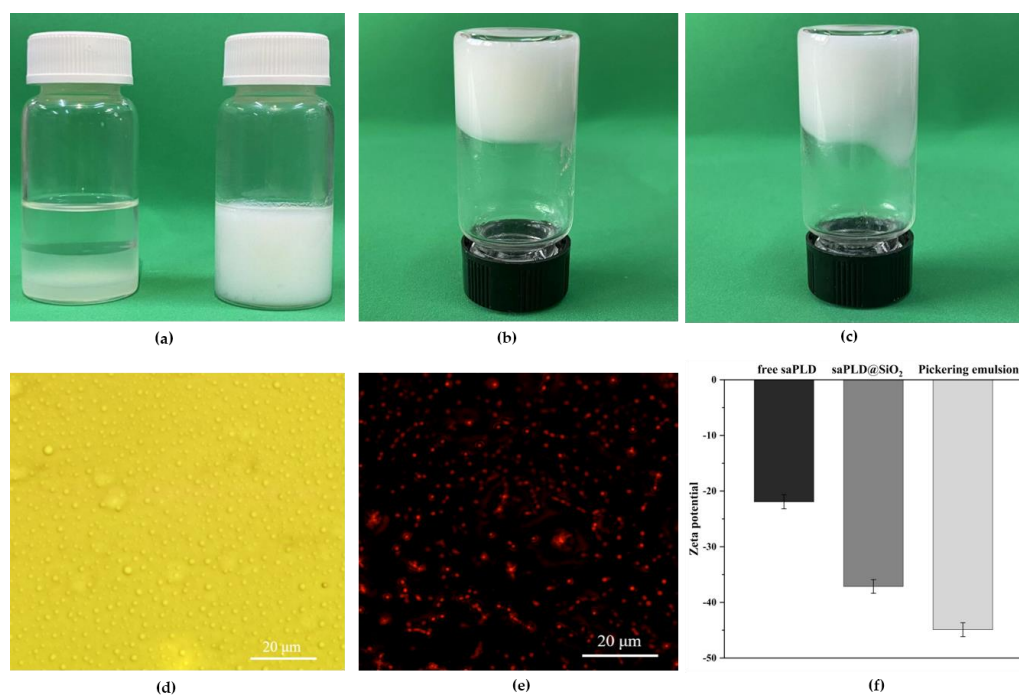


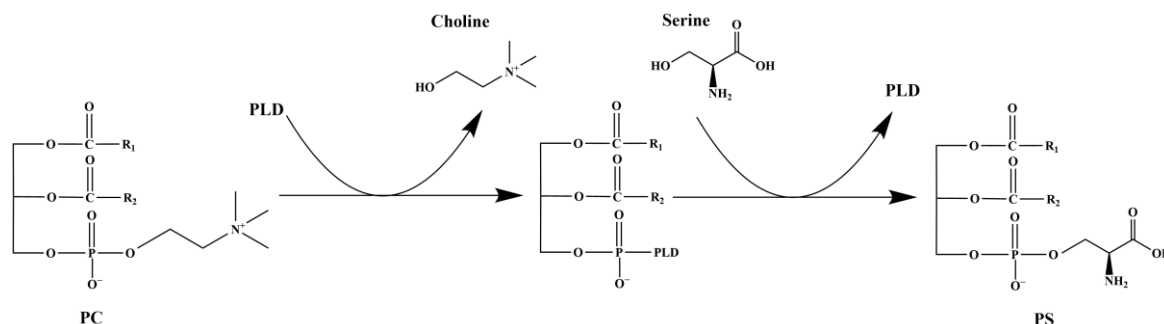
Figure 9. (a) Images of the aqueous and organic phases without sonication (left) and with sonication (right); (b) Emulsion appearance of Pickering emulsion; (c) Image of emulsion appearance after 7 days; (d) Image of Pickering emulsion; (e) Fluorescent image of the emulsion labeled with Nile red in the organic phase; (f) Zeta potential of Pickering emulsion, saPLD@SiO₂, and free saPLD. The data exhibited are the average values obtained from three paralleled experiments, while the error bars stand for the standard deviations.

In light of the titration experiments, the Pickering emulsion diffused in water and aggregated in oil, indicating that it was an oil-in-water emulsion. Additionally, the microscopy analysis of the Pickering emulsion exhibited a spherical structure of the droplets in the emulsion (Figure 9d), which is a typical droplet morphology of a Pickering emulsion. The oil phases were stained with Nile red to verify the type of emulsion [50], and the droplets showed a red fluorescence under the microscope, which confirmed the generation of an oil-in-water emulsion (Figure 9e). This oil-in-water emulsion might be capable of shortening the mass transfer distances, and, thus, each droplet could function as a microreactor to catalyze the production of PS from PC and L-serine.

To determine the surface charge and stability of the Pickering emulsion, the saPLD@SiO₂, and the free saPLD, a zeta potential analysis was performed. The value of the zeta potential is associated with the stability of particle dispersion, and it is a measure of the strength of the mutual attraction or repulsion among the particles, as follows: the smaller the dispersed particle or molecule is, the higher the absolute value of the zeta potential is, and, thus, the more stable the system, that is, the dispersion or dissolution can resist aggregation [51]. It is generally accepted that a stable system will be generated by a zeta potential higher than +30 mV or less than −30 mV [52]. As demonstrated in Figure 9f, the zeta potential value of the Pickering emulsion was −44.92 mV, which was much less than that of the saPLD@SiO₂ (−37.15 mV) or the free saPLD (−21.93 mV), and this phenomenon indicates that the Pickering emulsion was relatively stable, which might be beneficial to the transphosphatidylation reaction for the synthesis of PS from PC and L-serine.

2.7. Synthesis of Phosphatidylserine

The PLD-catalyzed synthesis of PS from soybean PC is based on a transphosphatidylation reaction, with PC as the donor of the phosphatidyl residue and L-serine as the acceptor [53]. The reaction scheme of the transphosphatidylation is shown in Scheme 2. However, the application of the free PLD as a biocatalyst is limited by its low productivity, high cost, and non-reusability. Moreover, transphosphatidylation is generally conducted in biphasic systems [54] (diethyl ether and aqueous solution), which might lead to a reduction in the enzyme activity and the denaturation of PLD. The small interfacial area drastically limits the response rate of biphasic systems, and Pickering emulsions exhibit several benefits when they are used in such systems, including non-pollution, higher stability, no negative effects on the enzyme activity, and ease of purification [55]. Pickering emulsions can enlarge the reaction interface area and shorten the mass transfer distance in order to increase biocatalysis in the biphasic system.



Scheme 2. The transphosphatidylation of the PLD.

According to Section 2.1, the saPLD@SiO₂ was prepared using saPLD and SiO₂ for biphasic reactions. The yield of PS was utilized to investigate the catalytic performance of the Pickering emulsion, the saPLD@SiO₂ (in a biphasic system), and the free saPLD (in a biphasic system). As demonstrated in Figure 10, the PS yield of the Pickering emulsion was 62% after 6 h, which was greater than that of the free saPLD and the saPLD@SiO₂ (18% and 41%, respectively). Compared to the free saPLD and saPLD@SiO₂ catalyst systems, the Pickering emulsion exhibited much greater efficiency to catalyze esterification, suggesting the general usefulness of this approach. Thus far, limited studies have been performed by combining immobilized enzymes to form a Pickering emulsion with the application of SiO₂ to immobilize PLD; thus, this work provides a competent platform for effective enzymatic catalysis in the biphasic system to synthesize PS.

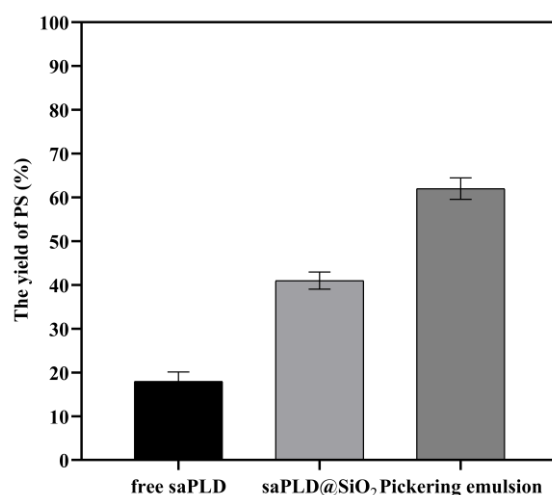


Figure 10. The PS yield of the Pickering emulsion, saPLD@SiO₂, and free saPLD. The data exhibited are the average values obtained from three paralleled experiments, while the error bars stand for the standard deviations.

3. Materials and Methods

3.1. Materials and Reagents

The soybean lecithin (PC content $\geq 90\%$) was supplied by Yuanye Bio (Shanghai, China). The L-serine was purchased from Solarbio Tech (Beijing, China). The PC ($\geq 99\%$, from soybean) and PS ($\geq 97\%$, from soybean) were obtained from Sigma-Aldrich (St. Louis, MO, USA). The ethyl propionate and SiO₂ were obtained from Macklin Biochemical Co., Ltd. (Shanghai, China). The saPLD was produced, purified, and then assayed, as previously described by Liu et al. [56].

3.2. Activity Assay of PLD

The activity of PLD to catalyze the transphosphatidylation was evaluated by analyzing the yield of PS from PC and L-serine. The reaction mixture was composed of 1 mL of 20-mM acetate/acetic acid buffer (pH 5.5) containing 0.06 g L-serine, 1 mL of ethyl propionate containing 0.025 g PC, and 500 μ L of saPLD. The reaction mixture was incubated for 20 min, with rapid shaking at 200 rpm and 40 °C, and then terminated by adding chloroform/methanol (2:1, *v/v*) solution (4 mL), followed by extracting the phospholipids. After centrifugation for 10 min at 8500 \times *g*, the lower layer was harvested and detected using high-performance liquid chromatography (HPLC).

The HPLC (Agilent Technologies, Palo Alto, CA, USA) analysis was conducted using a ZORBAX Rx-SIL silica gel column (5 μ m, 4.6 \times 250 mm, Agilent, Palo Alto, CA, USA) linked to an ultraviolet detector. The mobile phase was acetonitrile/methanol/phosphoric acid (95:5:0.8, *v/v/v*) and the flow rate was 0.3 mL/min. In addition, the column was incubated at 25 °C. The PS and PC were identified at 205 nm. One unit of PLD was designated as the quantity of enzymes producing 1 μ mol of PS from PC per min under the assay conditions.

3.3. Preparation of saPLD@SiO₂

The immobilization process was performed as follows: SiO₂ was first incubated with saPLD solution (20-mM Tris-HCl, pH 7.0) on a shaker, with shaking at 150 rpm, then, the mixture was washed with 20-mM Tris-HCl buffer (pH 7.0) at least two times to desorb the un-immobilized enzymes. The saPLD@SiO₂ was collected after centrifugation at 12,000 rpm for 1 min.

The immobilization was conducted with various enzyme contents (0.25, 0.5, 0.75, and 1.0 U) to investigate the influence of the enzyme amount. Then, the immobilization was performed under various temperatures (10, 20, 30, and 40 °C) to identify the effect of

immobilization temperature. Moreover, the immobilization was conducted in different timeframes (1, 2, 3, and 4 h) to determine the impact of immobilization time.

The favorable immobilization conditions for preparing saPLD@SiO₂ were identified by the relative enzyme activity and enzyme activity recovery rate. The enzyme activity recovery rate of saPLD@SiO₂ was described as the observed activity of immobilized enzymes divided by the total initial activity. The relative enzyme activity was the ratio (percentage) of the enzyme activity to the highest enzyme activity (marked as 100%).

3.4. Characterization of saPLD@SiO₂

3.4.1. Scanning Electron Microscopy

The surface morphologies of the saPLD@SiO₂ and SiO₂ were detected using scanning electron microscopy Apreo (SEM, Thermo Fisher Scientific, Waltham, MA, USA).

3.4.2. Confocal Laser Scanning Microscopy

The components of the saPLD@SiO₂ (saPLD and SiO₂) were labeled with different fluorescence. The saPLD was labeled with fluorescein isothiocyanate (FITC), which has a green fluorescence, and SiO₂ was labeled using rhodamine B (RB), which has a red fluorescence. Then, the saPLD@SiO₂ with fluorescence was detected using confocal laser scanning microscopy (CLSM, FV1000, Olympus, Tokyo, Japan).

3.4.3. Fourier Transform Infrared Spectroscopy

Fourier transform infrared spectroscopy (FT-IR) was utilized to identify the functional groups of saPLD@SiO₂ and SiO₂. The measurements were carried out via the KBr pressed-pellet method. Each sample was scanned with the FT-IR spectrophotometer (SENSOR, Bruker, Karlsruhe, Germany) at a range of 4000–400 cm⁻¹ wavenumbers.

3.5. Enzymatic Properties of saPLD@SiO₂

3.5.1. Optimum Temperatures and Thermal Stability

To investigate the influence of temperature on the saPLD@SiO₂ and free saPLD, the reactions were performed at various temperatures (40, 50, 60, 70, and 80 °C), and the enzyme activity was determined while keeping the other conditions unchanged. To determine the thermostability, the saPLD@SiO₂ and free saPLD were incubated without a substrate at different temperatures (40, 50, and 60 °C) for 1 h, and the residual activities of the saPLD@SiO₂ and free saPLD were recorded under standard assay conditions.

3.5.2. Optimum pH and pH Stability

To explore the optimum pH, the saPLD@SiO₂ and free saPLD activities were determined via the standard assay by incubating the reaction mixture at 40 °C with pH ranging from 5.0 to 9.0. To determine the pH stability, the saPLD@SiO₂ and free saPLD were incubated at 4 °C for 7 days at various pH (6.0, 7.0, and 8.0) in the absence of a substrate, then the residual activities were monitored under standard assay conditions.

3.6. Operational Stability of saPLD@SiO₂

The operational stability of the saPLD@SiO₂ was studied through the transphosphatidylolation reaction of L-serine and PC. In each reaction cycle, 0.1 g saPLD@SiO₂ was utilized to catalyze 0.2 g L-serine (in 5 mL of 20-mM acetate/acetic acid buffer (pH 5.5)) and 0.08 g PC (in 5 mL of ethyl propanoate) at 40 °C for 6 h. After each cycle, the saPLD@SiO₂ was immediately harvested by centrifugation (10,000 rpm, 2 min) and washed thrice using 20-mM acetate/acetic acid buffer (pH 5.5), and then used for the next round of catalytic reactions. For each batch cycle, the operational stability was obtained by comparing the relative PS yield with that of the first batch. The yield of PS was quantified by HPLC, with the approaches being noted in Section 3.2. The conversion rate (mol%) of PS was designated as the PS yield, which was calculated using the following equation: PS conversion rate (mol%) = PS amount/initial PC amount × 100%.

3.7. Storage Stability of saPLD@SiO₂

The storage stability of the saPLD@SiO₂ was detected by assessing the residual activity after 25 days of incubation in 20-mM Tris-HCl buffer (pH 7.0) at 4 °C, and the measurement of residual activity was conducted at a fixed time interval (every 5 days).

3.8. Preparation and Characterization of Pickering Emulsion

After washing with 20-mM Tris-HCl buffer (pH 7.0), the saPLD@SiO₂ (0.1 g) was mixed with 10 mL of ethyl propionate and prepared acetate/acetic acid buffer (20 mM, pH 7.0) (volume ratio of 1:1) to generate a mixture. Then, the mixture was subjected to ultrasound for 3 min at 40% intensity, with a 3-s ultrasound and a 3-s stand-by, which ultimately produced a stable Pickering emulsion.

The Pickering emulsion (1 mL) was added dropwise to 10 mL of organic solvent and 10 mL of water, and the type of emulsion was verified based on its aggregation and dispersion state. Then, the Pickering emulsion was placed in a 10-mL glass tube, which was kept vertical at 25 °C ± 2 °C. The stationary state stability of the Pickering emulsion was assessed for seven days after preparation by evaluating its visual appearance.

The Pickering emulsion was detected with an Olympus BX53 (Olympus Optical Co. Ltd., Tokyo, Japan) fluorescence microscope, and it was stained with Nile red, with an excitation wavelength of 488 nm and an emission wavelength of 539 nm. Additionally, the Pickering emulsion was detected using a bright-field microscope. A Zetasizer Nano ZS90 (Malvern Instrument, Malvern, UK) was used to detect the zeta potential of the Pickering emulsion, saPLD@SiO₂, and free saPLD.

3.9. Synthesis of Phosphatidylserine

The capacity of the Pickering emulsion or saPLD@SiO₂ (biphasic reaction systems) to synthesize PS from PC and L-serine was analyzed with free saPLD serving as a control.

The oil phase was composed of 5.0 mL of ethyl propionate containing 0.08 g PC, and the aqueous phase was composed of 5.0 mL of 20-mM acetate/acetic acid buffer (pH 7.0) with 0.2 g L-serine. Then, 0.1 g of saPLD@SiO₂ was added to initiate the reaction at 40 °C, with shaking at 200 rpm for 6 h. In addition, with the same amount of free saPLD serving as a control, the reaction system was the same as that of the saPLD@SiO₂, except the pH of the 20-mM acetate/acetic acid buffer (pH 6.0). The Pickering emulsion was prepared with the preceding emulsification procedure (Section 3.8). The reaction systems were kept at 40 °C, with shaking at 200 rpm for 6 h. Chloroform/methanol (2:1, *v/v*) solutions were mixed with the reaction mixture to extract PS and PC. After centrifugation at 8500 rpm for 10 min, the lower layer was harvested and detected using HPLC, as described in Section 3.2. The concentrations of phospholipids in the samples were acquired using the peak areas with standard curves, prepared by injecting phospholipid standards. The yield of PS was calculated according to Section 3.6.

4. Conclusions

In this study, we developed a strategy of immobilizing saPLD on the surface of SiO₂ through physical adsorption to successfully prepare the immobilized enzyme saPLD@SiO₂. The saPLD@SiO₂ also exhibited better thermostability and pH stability than the free saPLD. Additionally, the saPLD@SiO₂ demonstrated enhanced operational stability compared to free PLD, with good recyclability performance; furthermore, the relative yield remained over 50% for 14 consecutive batches. Moreover, a saPLD@SiO₂-stabilized Pickering emulsion was obtained by ultrasound, and the saPLD@SiO₂ at the organic–water interface enhanced the stability of the emulsion. Compared with the free saPLD and saPLD@SiO₂ in biphasic systems, the Pickering emulsion demonstrated an excellent catalytic performance in reactions of L-serine and PC, with the maximum conversion rate of 62% within 6 h. In summary, saPLD@SiO₂-stabilized Pickering emulsions could offer a novel strategy to efficiently produce PS.

Author Contributions: Conceptualization, H.S. and S.Z.; methodology, H.S., S.Z. and D.L.; formal analysis, H.S., S.Z., D.L., Z.H., Y.G. and J.H.; investigation, H.S., S.Z., D.L., Z.H., Y.G. and J.H.; writing—original draft preparation, H.S. and S.Z.; writing—review and editing, F.L. and Y.L.; supervision, Y.L.; project administration, Y.L.; funding acquisition, Y.L. All authors have read and agreed to the published version of the manuscript.

Funding: This work was supported by the National Natural Science Fund of China (32172156), the National Key Research and Development Program of China (2021YFC2100300), and the Tianjin Key-Training Program of “Project and Team” of China (XC202032).

Data Availability Statement: The data presented in this study are available on request from the corresponding author.

Conflicts of Interest: The authors declare no conflict of interest.

References

1. Zhou, W.B.; Gong, J.S.; Hou, H.J.; Li, H.; Lu, Z.M.; Xu, H.Y.; Xu, Z.H.; Shi, J.S. Mining of a phospholipase D and its application in enzymatic preparation of phosphatidylserine. *Bioengineered* **2018**, *9*, 80–89. [[CrossRef](#)] [[PubMed](#)]
2. Starks, M.A.; Starks, S.L.; Kingsley, M.; Purpura, M.; Jager, R. The effects of phosphatidylserine on endocrine response to moderate intensity exercise. *J. Int. Soc. Sports Nutr.* **2008**, *5*, 11. [[CrossRef](#)] [[PubMed](#)]
3. Fang, H.; Liu, A.; Dahmen, U.; Dirsch, O. Dual role of chloroquine in liver ischemia reperfusion injury: Reduction of liver damage in early phase, but aggravation in late phase. *Cell Death Dis.* **2013**, *4*, e694–e703. [[CrossRef](#)] [[PubMed](#)]
4. Ferreira, I.L.; Resende, R.; Ferreiro, E.; Rego, A.C.; Pereira, C.F. Multiple defects in energy metabolism in alzheimer’s disease. *Curr. Drug Targets* **2010**, *11*, 1193–1206. [[CrossRef](#)]
5. Zhang, Z.X.; Chen, M.; Xu, W.; Zhang, W.L.; Zhang, T.; Guang, C.E.; Mu, W.M. Microbial phospholipase D: Identification, modification and application. *Trends Food Sci. Technol.* **2020**, *96*, 145–156. [[CrossRef](#)]
6. Vance, J.E.; Tasseva, G. Formation and function of phosphatidylserine and phosphatidylethanolamine in mammalian cells. *Biochim. Biophys. Acta Mol. Cell Biol. Lipids* **2013**, *1831*, 543–554. [[CrossRef](#)]
7. Saeed, M.; van Brakel, M.; Zalba, S.; Schooten, E.; Rens, J.A.P.; Koning, G.A.; Debets, R.; ten Hagen, T.L.M. Targeting melanoma with immunoliposomes coupled to anti-MAGE A1 TCR-like single-chain antibody. *Int. J. Nanomed.* **2016**, *11*, 955–975. [[CrossRef](#)]
8. Delwaide, P.J.; Gyselynck-Mambourg, A.M.; Hurlet, A.; Yliff, M.J.A.N.S. Double-blind randomized controlled study of phosphatidylserine in senile demented patients. *Acta Neurol. Scand.* **2009**, *73*, 136–140. [[CrossRef](#)]
9. Liu, Y.H.; Huang, L.; Fu, Y.; Zheng, D.; Ma, J.Y.; Li, Y.Z.; Xu, Z.H.; Lu, F.P. A novel process for phosphatidylserine production using a *Pichia pastoris* whole-cell biocatalyst with overexpression of phospholipase D from *Streptomyces halstedii* in a purely aqueous system. *Food Chem.* **2019**, *274*, 535–542. [[CrossRef](#)]
10. Zhang, P.; Gong, J.S.; Qin, J.F.; Li, H.; Hou, H.J.; Zhang, X.M.; Xu, Z.H.; Shi, J.S. Phospholipids (PLs) know-how: Exploring and exploiting phospholipase D for its industrial dissemination. *Crit. Rev. Biotechnol.* **2021**, *41*, 1257–1278. [[CrossRef](#)]
11. Feng, X.X.; Yang, S.X.; Zhang, Y.H.; Zhiyuan, C.; Tang, K.Q.; Li, G.; Yu, H.; Leng, J.T.; Wang, Q.Y. GmPGL2, Encoding a pentatricopeptide repeat protein, is essential for chloroplast rna editing and biogenesis in soybean. *Front. Plant Sci.* **2021**, *12*, 690973. [[CrossRef](#)] [[PubMed](#)]
12. Duan, Z.Q.; Hu, F. Efficient synthesis of phosphatidylserine in 2-methyltetrahydrofuran. *J. Biotechnol.* **2013**, *163*, 45–49. [[CrossRef](#)] [[PubMed](#)]
13. Zhang, X.L.; Li, B.L.; Wang, J.; Li, H.Y.; Zhao, B.X. High-yield and sustainable production of phosphatidylserine in purely aqueous solutions via adsorption of phosphatidylcholine on Triton-X-100-modified silica. *J. Agric. Food Chem.* **2017**, *65*, 10767–10774. [[CrossRef](#)] [[PubMed](#)]
14. Selvy, P.E.; Lavieri, R.R.; Lindsley, C.W.; Brown, H.A. Phospholipase D: Enzymology, functionality, and chemical modulation. *Chem. Rev.* **2011**, *111*, 6064–6119. [[CrossRef](#)] [[PubMed](#)]
15. Shimbo, K.; Iwasaki, Y.; Yamane, T.; Ina, K.J.B. Purification and properties of phospholipase D from *Streptomyces antibioticus*. *Biosci. Biotechnol. Biochem.* **1993**, *11*, 1946–1948. [[CrossRef](#)]
16. Leiros, I.; McSweeney, S.; Hough, E. The reaction mechanism of phospholipase D from *Streptomyces sp* strain PMF. snapshots along the reaction pathway reveal a pentacoordinate reaction intermediate and an unexpected final product. *J. Mol. Biol.* **2004**, *339*, 805–820. [[CrossRef](#)]
17. Stieglitz, K.A.; Seaton, B.A.; Roberts, M.F. Proteolytically-clipped form of *S. chromofuscus* phospholipase D induces vesicle leakiness & enhances vesicle aggregation and fusion. *Biophys. J.* **2001**, *80*, 184A.
18. Hagishita, T.; Nishikawa, M.; Hatanaka, T. Isolation of phospholipase D producing microorganisms with high transphosphatidylase activity. *Biotechnol. Lett.* **2000**, *22*, 1587–1590. [[CrossRef](#)]
19. Diauddin, F.N.; Noor, S.A.M.; Rashid, J.I.A.; Knight, V.F.; Yunus, W.; Ong, K.K.; Kasim, N.A.M.; Taufik, S.; Samsuri, A.; Shamsudin, I.J.; et al. Preparation and characterisation of polypyrrole-iron oxyhydroxide nanocomposite as sensing material. *Adv. Mater. Sci. Eng.* **2020**, *2020*, 8762969. [[CrossRef](#)]

20. Chen, L.; Zou, M.; Hong, F.F. Evaluation of fungal laccase immobilized on natural nanostructured bacterial cellulose. *Front. Microbiol.* **2015**, *6*, 1245–1255. [[CrossRef](#)]
21. Bohari, N.A.; Shafiquzzaman, S.; Kamaruzaman, A.J.B. Development of formaldehyde biosensor for determination of formalin in fish samples; malabar red snapper (*Lutjanus malabaricus*) and longtail tuna (*Thunnus tonggol*). *Biosensors.* **2016**, *6*, 32. [[CrossRef](#)]
22. Chatzikonstantinou, A.V.; Gkantou, E.; Thomou, E.; Chalmpes, N.; Lyra, K.M.; Kontogianni, V.G.; Spyrou, K.; Patila, M.; Gournis, D.; Stamatis, H. Enzymatic Conversion of Oleuropein to Hydroxytyrosol Using Immobilized beta-Glucosidase on Porous Carbon Cuboids. *Nanomaterials* **2019**, *9*, 1166. [[CrossRef](#)] [[PubMed](#)]
23. Chen, K.; Liu, S.; Zhang, Q. Degradation and Detection of Endocrine Disruptors by Laccase-Mimetic Polyoxometalates. *Front. Chem.* **2022**, *10*, 854045. [[CrossRef](#)] [[PubMed](#)]
24. Bosio, V.E.; Islan, G.A.; Martinez, Y.N.; Duran, N.; Castro, G.R. Nanodevices for the immobilization of therapeutic enzymes. *Crit. Rev. Biotechnol.* **2016**, *36*, 447–464. [[CrossRef](#)]
25. Carvalho, N.B.; Vidal, B.T.; Barbosa, A.S.; Pereira, M.M.; Mattedi, S.; Freitas, L.D.; Lima, A.S.; Soares, C.M.F. Lipase immobilization on silica xerogel treated with protic ionic liquid and its application in biodiesel production from different oils. *Int. J. Mol. Sci.* **2018**, *19*, 1829. [[CrossRef](#)]
26. Miguel, S.; Legrand, G.; Duriot, L.; Delporte, M.; Menin, B.; Michel, C.; Olry, A.; Chataigne, G.; Salwinski, A.; Bygdell, J.; et al. A GDLS lipase-like from *Ipomoea batatas* catalyzes efficient production of 3,5-diCQA when expressed in *Pichia pastoris*. *Commun. Biol.* **2020**, *3*, 673–686. [[CrossRef](#)]
27. Fathi, Z.; Doustkhah, E.; Ebrahimpour, G.; Darvishi, F. Noncovalent immobilization of *Yarrowia lipolytica* lipase on dendritic-like amino acid-functionalized silica nanoparticles. *Biomolecules* **2019**, *9*, 502. [[CrossRef](#)]
28. Degorska, O.; Szada, D.; Zdarta, A.; Smulek, W.; Jesionowski, T.; Zdarta, J. Immobilized lipase in resolution of ketoprofen enantiomers: Examination of biocatalysts properties and process characterization. *Pharmaceutics* **2022**, *14*, 1443. [[CrossRef](#)]
29. Meir, I.; Alfassi, G.; Arazi, Y.; Rein, D.M.; Fishman, A.; Cohen, Y. Lipase Catalyzed Transesterification of model long-chain molecules in double-shell cellulose-coated oil-in-water emulsion particles as microbioreactors. *Int. J. Mol. Sci.* **2022**, *23*, 12122. [[CrossRef](#)]
30. Xi, Y.K.; Liu, B.; Wang, S.X.; Wei, S.H.; Yin, S.W.; Ngai, O.; Yang, X.Q. CO₂-responsive Pickering emulsions stabilized by soft protein particles for interfacial biocatalysis. *Chem. Sci.* **2022**, *13*, 2884–2890. [[CrossRef](#)]
31. Ren, G.H.; Li, Z.Z.; Lu, D.X.; Li, B.; Ren, L.L.; Di, W.W.; Yu, H.Q.; He, J.X.; Sun, D.J. pH and Magnetism dual-responsive pickering emulsion stabilized by dynamic covalent Fe₃O₄ nanoparticles. *Nanomaterials* **2022**, *12*, 2587. [[CrossRef](#)] [[PubMed](#)]
32. Dong, Z.; Liu, Z.S.; Shi, J.; Tang, H.; Xiang, X.; Huang, F.H.; Zheng, M.M. Carbon nanoparticle-stabilized pickering emulsion as a sustainable and high-performance interfacial catalysis platform for enzymatic esterification/transesterification. *ACS Sustain. Chem. Eng.* **2019**, *7*, 7619–7629. [[CrossRef](#)]
33. Pota, G.; Bifulco, A.; Parida, D.; Zhao, S.; Rentsch, D.; Amendola, E.; Califano, V.; Costantini, A. Tailoring the hydrophobicity of wrinkled silica nanoparticles and of the adsorption medium as a strategy for immobilizing lipase: An efficient catalyst for biofuel production. *Microporous Mesoporous Mater.* **2021**, *328*, 111504. [[CrossRef](#)]
34. Yang, T.; Thomas, A.M.; Dangi, B.B.; Kaiser, R.I.; Mebel, A.M.; Millar, T.J. Directed gas phase formation of silicon dioxide and implications for the formation of interstellar silicates. *Nat. Commun.* **2018**, *9*, 774–782. [[CrossRef](#)] [[PubMed](#)]
35. Mao, S.H.; Zhang, Z.H.; Ma, X.Y.; Tian, H.; Lu, F.P.; Liu, Y.H. Efficient secretion expression of phospholipase D in *Bacillus subtilis* and its application in synthesis of phosphatidylserine by enzyme immobilization. *Int. J. Biol. Macromol.* **2021**, *169*, 282–289. [[CrossRef](#)] [[PubMed](#)]
36. Younus, H.; Rajcani, J.; Ulbrich-Hofmann, R.; Saleemuddin, M. Behaviour of a recombinant cabbage (*Brassica oleracea*) phospholipase D immobilized on CNBr-activated and antibody supports. *Biotechnol. Appl. Biochem.* **2004**, *40*, 95–99. [[CrossRef](#)]
37. Islam, M.M.; Chakraborty, M.; Pandya, P.; Al Masum, A.; Gupta, N.; Mukhopadhyay, S. Binding of DNA with Rhodamine B: Spectroscopic and molecular modeling studies. *Dye. Pigment.* **2013**, *99*, 412–422. [[CrossRef](#)]
38. Potter, M.N.; Green, J.R.; Mutus, B. Fluorescein isothiocyanate, a platform for the selective and sensitive detection of S-Nitrosothiols and hydrogen sulfide. *Talanta* **2022**, *237*, 122981–122988. [[CrossRef](#)]
39. Shabanian, M.; Hajibeygi, M.; Raeisi, A. FTIR Characterization of Layered Double Hydroxides and Modified Layered Double Hydroxides. In *Layered Double Hydroxide Polymer Nanocomposites*; Elsevier: Amsterdam, The Netherlands, 2020; pp. 77–101.
40. Califano, V.; Costantini, A.; Silvestri, B.; Venezia, V.; Cimino, S.; Sannino, F. The effect of pore morphology on the catalytic performance of β-glucosidase immobilized into mesoporous silica. *Pure Appl. Chem.* **2019**, *91*, 1583–1592. [[CrossRef](#)]
41. Ha Li, S.S.; Li, Y.; Long, N.B.; Jiang, F.; Zhang, R.F. Highly active and stable nanobiocatalyst based on in-situ cross-linking of phospholipase D for the synthesis of phosphatidylserine. *Int. J. Biol. Macromol.* **2018**, *117*, 1188–1194. [[CrossRef](#)]
42. Zhao, X.; Guo, M.; Li, X.; Liu, B.; Li, B.; Wang, J. Immobilization of Bio-imprinted Phospholipase D and Its Catalytic Behavior for Transphosphatidylation in the Biphasic System. *Appl. Biochem. Biotechnol.* **2023**. [[CrossRef](#)] [[PubMed](#)]
43. Han, Q.Q.; Zhang, H.Y.; Sun, J.A.; Liu, Z.; Huang, W.C.; Xue, C.H.; Mao, X.Z. Immobilization of phospholipase D on silica-coated magnetic nanoparticles for the synthesis of functional phosphatidylserine. *Catalysts* **2019**, *9*, 361. [[CrossRef](#)]
44. Li, Y.; Wu, J.Q.; Long, N.B.; Zhang, R.F. Efficient immobilization of phospholipase D on novel polymer supports with hierarchical pore structures. *Int. J. Biol. Macromol.* **2019**, *141*, 60–67. [[CrossRef](#)] [[PubMed](#)]
45. Sanchez-Salvador, J.L.; Balea, A.; Monte, M.C.; Blanco, A.; Negro, C. Pickering emulsions containing cellulose microfibers produced by mechanical treatments as stabilizer in the food industry. *Appl. Sci.* **2019**, *9*, 359. [[CrossRef](#)]

46. de Carvalho-Guimaraes, F.B.; Correa, K.L.; de Souza, T.P.; Amado, J.R.R.; Ribeiro-Costa, R.M.; Silva, J.O.C. A Review of Pickering Emulsions: Perspectives and Applications. *Pharmaceuticals* **2022**, *15*, 1413. [[CrossRef](#)] [[PubMed](#)]
47. Chen, L.J.; Ao, F.; Ge, X.M.; Shen, W. Food-Grade Pickering Emulsions: Preparation, Stabilization and Applications. *Molecules* **2020**, *25*, 3202. [[CrossRef](#)] [[PubMed](#)]
48. Yang, H.L.; Cai, W.B.; Lv, W.; Zhao, P.; Shen, Y.M.; Zhang, L.F.; Ma, B.; Yuan, L.J.; Duan, Y.Y.; Yao, K.C. A new strategy for accurate targeted diagnosis and treatment of cutaneous malignant melanoma: Dual-mode phase-change lipid nanodroplets as ultrasound contrast agents. *Int. J. Nanomed.* **2019**, *14*, 7079–7093. [[CrossRef](#)]
49. Wang, S.R.; Wang, T.Y.; Li, X.Y.; Cui, Y.J.; Sun, Y.; Yu, G.P.; Cheng, J.J. Fabrication of emulsions prepared by rice bran protein hydrolysate and ferulic acid covalent conjugate: Focus on ultrasonic emulsification. *Ultrason. Sonochem.* **2022**, *88*, 106064–106074. [[CrossRef](#)]
50. Zhang, T.T.; Jiang, H.; Hong, L.Z.; Ngai, T. Multiple Pickering emulsions stabilized by surface-segregated micelles with adaptive wettability. *Chem. Sci.* **2022**, *13*, 10752–10758. [[CrossRef](#)]
51. Tng, D.J.H.; Song, P.Y.; Lin, G.M.; Soehartono, A.M.; Yang, G.; Yang, C.B.; Yin, F.; Tan, C.H.; Yong, K.T. Synthesis and characterization of multifunctional hybrid-polymeric nanoparticles for drug delivery and multimodal imaging of cancer. *Int. J. Nanomed.* **2015**, *10*, 5771–5786. [[CrossRef](#)]
52. Foroushani, P.H.; Rahmani, E.; Alemzadeh, I.; Vossoughi, M.; Pourmadadi, M.; Rahdar, A.; Diez-Pascual, A.M. Curcumin Sustained Release with a Hybrid Chitosan-Silk Fibroin Nanofiber Containing Silver Nanoparticles as a Novel Highly Efficient Antibacterial Wound Dressing. *Nanomaterials* **2022**, *12*, 3426. [[CrossRef](#)] [[PubMed](#)]
53. Arora, H.; Culler, M.D.; Decker, E.A. Production of a High-phosphatidylserine lecithin that synergistically inhibits lipid oxidation with alpha-tocopherol in oil-in-water emulsions. *Foods* **2022**, *11*, 1014. [[CrossRef](#)] [[PubMed](#)]
54. Hu, R.K.; Cui, R.G.; Lan, D.M.; Wang, F.H.; Wang, Y.H. Acyl chain specificity of marine *streptomyces klenkii* phospholipase D and its application in enzymatic preparation of phosphatidylserine. *Int. J. Mol. Sci.* **2021**, *22*, 10580. [[CrossRef](#)]
55. Mable, C.J.; Warren, N.J.; Thompson, K.L.; Mykhaylyk, O.O.; Armes, S.P. Framboidal ABC triblock copolymer vesicles: A new class of efficient Pickering emulsifier. *Chem. Sci.* **2015**, *6*, 6179–6188. [[CrossRef](#)] [[PubMed](#)]
56. Liu, Y.H.; Lu, F.P.; Chen, G.Q.; Snyder, C.; Sun, J.; Li, Y.; Wang, J.L.; Xiao, J. High-level expression, purification and characterization of a recombinant medium-temperature alpha-amylase from *Bacillus subtilis*. *Biotechnol. Lett.* **2010**, *32*, 119–124. [[CrossRef](#)]

Disclaimer/Publisher’s Note: The statements, opinions and data contained in all publications are solely those of the individual author(s) and contributor(s) and not of MDPI and/or the editor(s). MDPI and/or the editor(s) disclaim responsibility for any injury to people or property resulting from any ideas, methods, instructions or products referred to in the content.